PSMB8 Encoding the β5i Proteasome Subunit Is Mutated in Joint Contractures, Muscle Atrophy, Microcytic Anemia, and Panniculitis-Induced Lipodystrophy Syndrome

Anil K. Agarwal,[1] Chao Xing,[2] George N. DeMartino,[3] Dario Mizrachi,[4] Maria Dolores Hernandez,[5] Ana Berta Sousa,[6] Laura Martínez de Villarreal,[5] Heloísa G. dos Santos,[6] and Abhimanyu Garg[1,*]

We performed homozygosity mapping in two recently reported pedigrees from Portugal and Mexico with an autosomal-recessive autoinflammatory syndrome characterized by joint contractures, muscle atrophy, microcytic anemia, and panniculitis-induced lipodystrophy (JMP). This revealed only one homozygous region spanning 2.4 Mb (5818 SNPs) on chromosome 6p21 shared by all three affected individuals from both families. We directly sequenced genes involved in immune response located in this critical region, excluding the HLA complex genes. We found a homozygous missense mutation c.224C>T (p.Thr75Met) in the proteasome subunit, beta-type, 8 (*PSMB8*) gene in affected patients from both pedigrees. The mutation segregated in an autosomal-recessive fashion and was not detected in 275 unrelated ethnically matched healthy subjects. *PSMB8* encodes a catalytic subunit of the 20S immunoproteasomes called β5i. Immunoproteasome-mediated proteolysis generates immunogenic epitopes presented by major histocompatibility complex (MHC) class I molecules. Threonine at position 75 is highly conserved and its substitution with methionine disrupts the tertiary structure of PSMB8. As compared to normal lymphoblasts, those from an affected patient showed significantly reduced chymotrypsin-like proteolytic activity mediated by immunoproteasomes. We conclude that mutations in *PSMB8* cause JMP syndrome, most probably by affecting MHC class I antigen processing.

We recently reported a distinct autosomal-recessive syndrome presenting with joint contractures, muscle atrophy, microcytic anemia, and panniculitis-induced childhood-onset lipodystrophy (JMP) in three patients from two pedigrees.[1] The lipodystrophy affected the face, arms, and thorax initially and more severely than the abdomen and lower extremities, which were affected later (Figure S1 available online). Although the patients did not have acanthosis nigricans, diabetes, or hyperinsulinemia, mild metabolic disturbances such as borderline hypertriglyceridemia, markedly low levels of high-density lipoprotein cholesterol, and mild elevations of liver enzymes were noted. All the patients had hepato-splenomegaly and hypergammaglobulinemia. Joint contractures initially affected the hands and feet, which were more severely deformed than the other joints.

Similar manifestations have been reported previously from Japan in three patients who in addition presented with fever, elevated erythrocyte sedimentation rate, macroglossia, mental retardation, and calcification of basal ganglia.[2–5] The genetic basis of the JMP syndrome was unknown and we had hypothesized that it belongs to the group of inherited autoinflammatory diseases.[6] By using genome-wide homozygosity mapping, we now report a homozygous missense mutation in the proteasome subunit, β-type, 8 (*PSMB8* [MIM 177046]) gene, which encodes the β5i subunit (also known as large multifunctional protease 7, LMP7), a catalytic subunit of immunoproteasomes in patients with JMP syndrome.

Affected individuals and their family members were recruited into our ongoing study of genetic basis of lipodystrophies (Figure S2). The protocol was approved by the Institutional Review Board of UT Southwestern and Hospital de Santa Maria, and all the patients, their family members, and healthy controls gave the written informed consent.

Genomic DNA was extracted from buffy coat or from Epstein-Barr virus-transformed lymphoblastoid cell lines via the Easy-DNA kit (Invitrogen, Carlsbad, CA). Genotyping was performed with the Illumina HumanOmni1-Quad Beadchip by the Microarray Core Facility at UT Southwestern. Allele calls were generated with GenomeStudio version 1.5.16. Consanguinity was confirmed in family JMP100 and suspected in family JMP200, suggesting a recessive disease. Therefore, we carried out both classic homozygosity mapping via linkage analysis[7] and modern homozygosity mapping via identifying regions of extended homozygosity. We chose 7296 single-nucleotide polymorphisms (SNPs) from among the ~1 million SNPs from the HumanOmni1-Quad chip to construct a sparse linkage map, in which SNPs were spaced ~2 per centiMorgan. In family JMP200, we performed linkage analysis with the sparse map under a recessive model by assuming individuals JMP200.1 and JMP200.2 were first cousins, as proposed by Hildebrandt et al.[8] The analysis was done

[1]The Division of Nutrition and Metabolic Diseases, Department of Internal Medicine and the Center for Human Nutrition, University of Texas Southwestern Medical Center, Dallas, TX 75390, USA; [2]Department of Clinical Sciences, University of Texas Southwestern Medical Center, Dallas, TX 75390, USA; [3]Department of Physiology, University of Texas Southwestern Medical Center, Dallas, TX 75390, USA; [4]Division of Endocrinology, Department of Internal Medicine, University of Texas Southwestern Medical Center, Dallas, TX 75390, USA; [5]Departamento de Genética, Facultad de Medicina, Universidad Autonoma de Nuevo Leon, Monterrey, Nuevo León, 66603, México; [6]Serviço de Genética Médica, Hospital de Santa Maria, 1649-035 Lisbon, Portugal
*Correspondence: abhimanyu.garg@utsouthwestern.edu
DOI 10.1016/j.ajhg.2010.10.031.

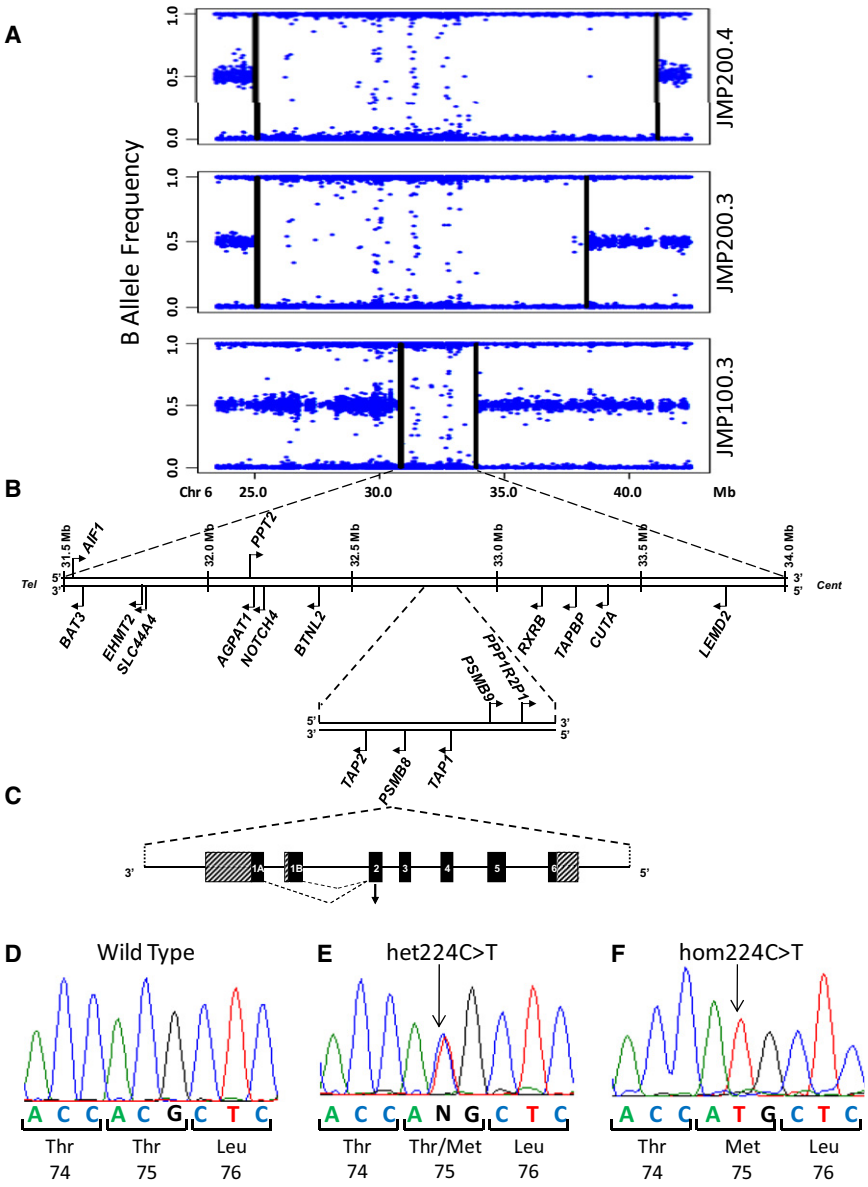

Figure 1. Homozygous Region Shared by Affected Individuals with JMP Syndrome, Position of Candidate Genes in the Region, Structure of *PSMB8*, and Disease-Causing Mutation

(A) Homozygous region shared by the affected individuals JMP 200.4, 200.3, and 100.3. The B allele frequency is a normalized measure of the allelic intensity ratio of the two alleles, and deviation from 0.5 indicates homozygosity. The genomic position is based on NCBI36/hg18 assembly. Each dot indicates the SNP genotyped by means of the Illumina HumanOmni1-Quad Beadchip. The vertical lines for each panel indicate the regions of homozygosity. Isolated heterozygous SNPs within larger homozygous segments are likely to represent miscalls.

(B) Position of some of the candidate genes in the critical region identified by homozygosity mapping. Tel, telomeric end; cent, centromeric end. The critical region spanned from 31.5 Mb to 34.0 Mb on chromosome 6.

(C) Structure of *PSMB8* and the location of the mutation in the JMP patients. Human *PSMB8* contains six exons and five introns. Also shown are the alternatively spliced exons 1A and 1B. The mutation c.224C>T in *PSMB8* is located in exon 2.

(D) Sequence electropherogram for normal sequence in exon 2 of *PSMB8*.

(E) Sequence from JMP 200.2 showing heterozygous c.224C>T mutation.

(F) Sequence from JMP 200.3 showing the homozygous c.224C>T mutation. The amino acid substitution is shown below the electropherogram.

with MERLIN.[9] We also screened for regions of extended homozygosity in all individuals via PLINK.[10]

The genome-wide linkage scan in family JMP200 identified only one region on 6p21 spanning ~16.7 Mb (~13.4 cM) with a positive lod score of 0.93 (Figure S3). Across the genome, there was only one homozygous region spanning 2.4 Mb (5818 SNPs) shared by all three affected individuals from both families (Figure 1A) but not by any unaffected. This homozygous region was located under the linkage peak. There was no indication of copy number variation in the region according to the Log R Ratio. Excluding the HLA complex, ~200 genes are located within this region, including those that are predicted or are of unknown function. Because we had hypothesized that the JMP syndrome is an autoinflammatory syndrome, we initially selected genes that might affect the immune response (Figure 1B). These included *PSMB8* and *PSMB9* (proteasomal subunits also called β5i and β1i, respectively; MIM 177046 and 177045, respectively), *TAP1* and *TAP2* (transporters 1 and 2, ATP-binding cassette, subfamily B associated with antigen processing; MIM 170260 and 170261, respectively), and *TAPBP* (TAP binding protein; MIM 601962). We also selected *PBX2* (pre-B cell leukemia homeobox 2, a transcription factor; MIM 176311), *BTNL2* (butyrophilin-like 2, a member of the B7 family of costimulatory molecules; MIM 606000), *AIF1* (allograft inflammatory factor 1, which is associated with rheumatoid arthritis; MIM 601833), and *AGPAT1* (acylglycerol phosphate acyltransferase, isoform 1, involved in triglyceride biosynthesis; MIM 603099). The coding regions and the splice site junctions of the genes in the critical region were amplified with gene-specific primers located in intronic regions (Table S1). Polymerase chain reaction (PCR) was assembled as described earlier.[11] The PCR product was purified to remove primers and dNTPs and sequenced with ABI Prism 3100.

We found a homozygous c.224C>T mutation in *PSMB8* (NM_148919.3; MIM 177046) in the affected subjects from both pedigrees (Figures 1C–1F). This mutation is predicted

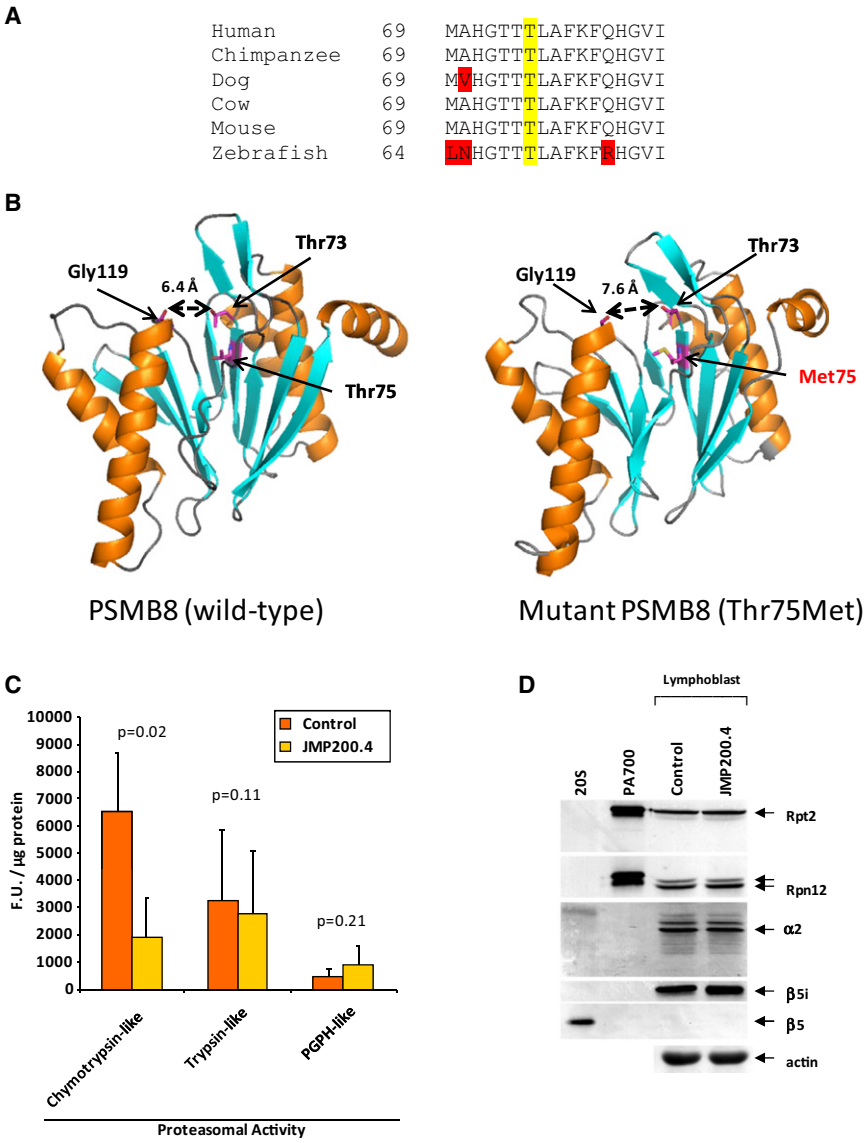

Figure 2. Conservation of the Mutated Residue across Species, Crystal Structure of Normal and Mutant PSMB8, Proteasomal Activity, and Expression of β5i in Cell Lysates of Lymphoblasts from an Affected Patient

(A) Alignment of partial PSMB8 amino acid sequence around threonine at position 75 in human (NP_683720.2), chimpanzee (XP_001167272.1), dog (XP_532100.1), cow (NP_001035570.1), mouse (NP_034854.1), and zebrafish (NP_571467.2). The conserved residue threonine is highlighted in yellow. Amino acids that are not conserved are shown in red.

(B) Protein model for the wild-type and mutant, Thr75Met, human PSMB8. β sheets are shown in blue, helices in orange, and unstructured loops in gray. Threonine 73 and glycine 119 are the catalytic amino acids. Mutation of threonine 75 to methionine widens the distance between the catalytic threonine 73 and glycine 119 by 1.2 Å. All amino acids are numbered according to transcript 1B.

(C) Proteasomal activity in EBV-transformed lymphoblasts from a control and an affected patient (JMP200.4). The chymotrypsin-like, trypsin-like, and PGPH-like proteolytic activities are expressed as fluorogenic units (F.U.) per µg of protein. Each bar represents mean ± SD from three independent experiments carried out in duplicate. p values were derived from the paired t test.

(D) Western blots. Total cell lysates from EBV-transformed lymophoblasts of a control subject and an affected patient (JMP200.4) were resolved on 10% SDS-PAGE and probed with antibodies against Rpt2 (an ATPase of the PA700, a 19S proteasome regulatory particle), Rpn12 (a subunit of 19S proteasome regulatory subunit), α2, β5i, and β5 (subunits of 20S proteasome), and a housekeeping protein actin. The first two lanes on the left contain purified 20S and PA700 proteins from bovine red blood cells as positive controls. The control and the patient contained the same amount of β5i protein.

to result in substitution of threonine at position 75 with methionine (p.Thr75Met; numbering according to transcript 1B; NP_683720.2). The available parents and unaffected siblings harbored the heterozygous mutation. No other disease-causing variant was found on sequencing of candidate genes in the region (Table S2). Genotyping DNA of 275 healthy ethnically matched subjects of Hispanic origin from Dallas revealed no one harboring the c.224C>T variant in *PSMB8*. We aligned genotypes of the three affected from both families in the homozygous region and identified a segment of 0.22 Mb covering *PSMB8* shared by all three affected (Table S3). This suggests that the haplotypes shared by the affected subjects in both families are identical-by-descent; however, the origin of the mutation seems to be ancient.

The threonine at position 75 of PSMB8 is highly conserved across species (Figure 2A). Prediction of the structure and conserved regions between highly homologous (>75%) human PSMB8 (protein ID NP_683720.2) and yeast PSMB5 (ortholog of human β5, protein ID NP_015428.1) via Clustal W analysis allowed us to manually exchange the amino acids in yeast PSMB5 (PDB identification number 1z7q, chain L)[12,13] with those represented exclusively in human PSMB8 via the PyMol program (PyMOL Molecular Graphics System, Version 1.2r3pre, Schrödinger, LLC). For further optimization protocol, we used multiple step energy minimization and molecular dynamics (MD) simulation to fully relax our initial model. All simulations were carried out with the Amber 9 program[14] with force field (ff99) and periodic

boundary conditions.[15] To simulate behavior in solution, the protein was solvated with a 10 Å TIP3P octagon water cap. Prior to MD simulations, two steps of minimization were performed. First, the human PSMB8 was fixed and only the positions occupied by water were minimized followed by the minimization of the entire simulation system. After energy minimization, a 100 picosecond MD simulation was carried out under constant volume conditions, and temperature was heated up continuously from 0°K to 300°K. The time step of the simulations was 2.0 femtoseconds with a cutoff of 12 Å for nonbonded interactions. The final conformations were obtained when the total energy reached the minimum. The best structure was examined with the Profile-3D[16] and Procheck[17] programs. Protein modeling of the Thr75Met substitution showed that it relaxes PSMB8 by 1.2 Å and may affect the proteolytic processing of peptides (Figure 2B).

Proteasome activity was determined in the cell lysates of Epstein-Barr virus-transformed lymphoblasts from a control subject and an affected patient (JMP200.4). Lymphoblasts were washed with PBS, pelleted by centrifugation, and lysed in four volumes of buffer consisting of 50 mM Tris-HCl (pH 7.8), 5 mM 2-mercaptoethanol, 1 mM ATP, and 5 mM $MgCl_2$. Lysates were cleared of cell debris by centrifugation at 5000 × g for 5 min. Proteasome activity was determined by hydrolysis of peptide substrates as described previously.[18] We employed three different peptides that are specific, preferred substrates for three classes of peptidases having chymotrypsin-like, trypsin-like, and peptidyl glutamyl peptide-hydrolyzing (PGPH) activity. In brief, cell extracts were incubated with 50 μM substrates (succinyl-Leu-Leu-Val-Tyr-7-amino-4-methylcoumarin, succinyl-Val-Leu-Arg-7-amino-4-methylcoumarin, or benzyloxycarbonyl-Leu-Leu-Glu-7-amino-4-methylcoumarin) for 20 min at 37°C. The rate of amino-4-methylcoumarin production, a direct measure of proteasome activity, was monitored continuously by fluorescence detection at 360 nm excitation/480 nm emission, with a BioTek Synergy MX Plate reader. Steady-state rates of proteolysis were expressed as arbitrary fluorescence units produced per min of incubation and were normalized per μg of protein. Protein concentration was determined with the Bradford method.[19] We observed markedly reduced chymotrypsin-like activity but not trypsin-like or PGPH-like activity in lymphoblast cell lysates from the patient with JMP syndrome (Figure 2C). A marked reduction in the proteasomal activity was observed in the presence of MG132, a specific inhibitor of S26 proteasomes, when tested with substrate succinyl-Leu-Leu-Val-Tyr-7-amino-4-methylcoumarin, consistent with the presence of proteasomal activity (Figure S4). This observation was further confirmed by determining the presence of key subunits of proteasome/immunoproteasome by western blots. For western blotting, 40 μg of total cellular protein from lymphoblast cell lysates from the patient and control was resolved on 10% SDS-PAGE and transferred to nitrocellulose membranes for immunoblotting with various primary antibodies against Rpt2 (an ATPase of the PA700, a 19S proteasome regulatory particle), Rpn12 (a subunit of 19S proteasome regulatory subunit), and α2, β5i, and β5 (subunits of 20S proteasome). All of the antibodies were raised in-house as described previously,[18,20] detected with peroxidase-labeled secondary antibody, and exposed to X-ray film. β-actin was used as a housekeeping gene and loading control. No difference was observed in the expression of various components of the proteasomal units, including β5i subunit in the cell lysates from the control and patient (Figure 2D).

Table 1. Serum Cytokine Levels in Affected Patients

Serum Cytokine	JMP 200.3	JMP 200.4	Reference Intervals in (pg/mL)
IL-1β	27	18	0–36
IL-2	8	<5	0–12
IL-2 receptor	806	**1316**	0–1033
IL-4	**6**	<5	0–5
IL-5	**6**	5	0–5
IL-6	**37**	**79**	0–5
IL-8	**46**	**8**	0–5
IL-10	9	18	0–18
IL-12	**8**	6	0–6
IL-13	<5	<5	0–5
Interferon-γ	**14**	**17**	0–5
TNF-α	6	<5	0–22

IL, interleukin; TNF, tumor necrosis factor. Abnormally high levels are indicated in bold.

Therefore, this study suggests that a homozygous missense loss-of-function mutation in *PSMB8* causes the JMP syndrome. This conclusion is supported by the following observations: (1) evidence of linkage to the 6p21.2 region and homozygosity in the same region; (2) a homozygous c.224C>T missense variant in *PSMB8* in the two pedigrees; (3) segregation of the c.224C>T mutation in other members of the pedigrees in an autosomal-recessive fashion; (4) no previous report of this variant as a SNP in any database; (5) lack of this variant in ethnically matched healthy controls; (6) substitution of methionine for the highly conserved threonine at position 75 of PSMB8 disrupts the tertiary structure of the protein; and (7) reduced chymotrypsin-like proteasomal activity in cell lysates of lymphoblasts from an affected patient.

To gain insight into the functional effects of the p.Thr75Met variant, we measured serum interleukin (IL) 1β, 2, 4, 5, 6, 8, 10, 12, IL-2 receptor, interferon-γ, and tumor necrosis factor-α (ARUP Laboratories, Salt Lake City, UT) in two affected patients from JMP200 pedigree, which revealed that both affected patients had 7- to 19-fold increased levels of IL-6 and 2.8- to 3.5-fold elevated levels of interferon γ (Table 1). Whereas serum levels of

IL-8 were >9-fold elevated in JMP 200.3, in JMP200.4 only 1.6-fold elevation was observed. The levels of other cytokines were not elevated in both patients. Marked elevation of erythrocyte sedimentation rate and serum γ globulins, interferon-γ, and IL-6 levels without elevation in other cytokines such as IL-1 and TNF-α suggest not only an ongoing inflammation but also a peculiar biomarker signature present in the JMP syndrome. Ongoing inflammation was clearly evident in the patient JMP200.4 who had many active skin lesions at the time of examination (Figure S1), which were biopsy proven to be consistent with panniculitis.

PSMB8 encodes β5i, a catalytic subunit of the immunoproteasome.[21] Immunoproteasome-mediated proteolysis generates immunogenic epitopes presented by major histocompatibility complex (MHC) class I molecules. This degradation follows covalent modification of the proteins with polyubiquitin,[22,23] which targets them to the 26S proteasome. The 26S proteasome is composed of two subcomplexes: the 20S proteasome that contributes protease function and PA700 (19S regulator) that mediates translocation of the attached substrates to the 20S proteasome. The 20S proteasome is a 700,000 dalton complex composed of four axially stacked heptameric rings. Each of the two identical outer rings contains seven different α type subunits, and each of the two identical inner rings contains seven different β type subunits.[23] The β1, β2, and β5 subunits display different specificities for peptide bond hydrolysis and have predominantly PGPH-, trypsin-, and chymotrypsin-like activities, respectively.[22,24] Higher eukaryotes contain isoforms of β1, β2, and β5, termed β1i, β2i, and β5i, respectively, which are selectively incorporated into immunoproteasomes. Immunoproteasomes are constitutively expressed in cells of hematopoietic origin, particularly lymphocytes and monocytes, but can be induced in nonhematopoietic cells after exposure to inflammatory cytokines such as interferon-γ.[21] Proteasomes and immunoproteasomes are functionally very similar, but not identical. Immunoproteasomes stimulate cleavage after hydrophobic, basic, and branched chain residues, while suppressing cleavage after acidic residues,[25–27] and thus can potentially enhance the generation of some antigenic epitopes differently from the proteasomes. However, a clear distinction of the role of proteasomes and immunoproteasomes in immune response has not yet emerged.

Targeted gene deletion of *Psmb8* in mice causes reduced MHC class I cell surface expression and inefficient presentation of the endogenous male antigen HY.[28] These mice are healthy, have normal T and B lymphocyte counts in their lymphoid organs,[28] and respond normally to challenge with lymphocytic choriomeningitis virus,[29] but are susceptible to infection with *Toxoplasma gondii*.[30] The patients with JMP syndrome, however, are not known to be prone to infections. The lack of resemblance of the phenotype of $Psmb8^{-/-}$ mice to that observed in patients with JMP syndrome may indicate different biology of the PSMB8 in humans and mice. Further to this, our patients have only missense mutation, whereas in the mice the whole gene is deleted. Nonetheless, further studies are required to fully understand the underlying reasons for discrepancy in the phenotype of patients with JMP syndrome and $Psmb8^{-/-}$ mice.

Recently, studies with PR-957, a selective inhibitor of β5i (LMP7) that binds to the active site and specifically inhibits chymotrypsin-like peptidase activity, have revealed a unique role of PSMB8 in cytokine production.[31] In endotoxin-stimulated peripheral blood mononuclear cells from healthy subjects and from patients with rheumatoid arthritis, PR-957 blocked production of IL-23 by ~80% and of TNF-α and IL-6 by ~50%.[31] Further, PR-957 ameliorated disease in two mouse models of arthritis.[31] However, our patients had hypergammaglobulinemia and extremely high serum levels of IL-6 and interferon-γ. These data suggest that p.Thr75Met substitution may have additional effects beyond a partial loss of function. This substitution may alter the processing of an exogenous or endogenous antigen so as to trigger an accelerated immune response targeted most directly to adipose tissue, joints, and muscles.

So far, the monogenic autoinflammatory diseases have been reported to be due to mutations in the family of PYRIN domain-containing proteins, proteins interacting with pyrin, and others, resulting in activation of the interleukin-1β pathway.[6] This report expands the spectrum of autoinflammatory diseases to include JMP syndrome resulting from altered immunoproteasome function. How reduced chymotrypsin-like proteasomal activity resulting from a loss-of-function *PSMB8* mutation results in joint contractures, panniculitis-induced lipodystrophy, and the other clinical features of JMP syndrome remains to be elucidated.

Supplemental Data

Supplemental Data include four figures and three tables and can be found with this article online at http://www.cell.com/AJHG/.

Acknowledgments

We thank Sarah Masood and Katie Tunison for help with illustrations and mutational screening; Shyam Murali, Prateek Sharma, and Marquis Harris for sequencing candidate genes in the critical region; Helen Hobbs, M.D., for providing DNA samples of the Hispanic controls; Tommy Hyatt for genotyping; Laurie Davis, Ph.D., for providing control lymphoblasts; David Thompson for help with the proteasomal activity assay; Beverley Adams-Huet, M.S., for statistical analysis; Andrew Zinn, M.D., Ph.D., for helpful suggestions; and Michael S. Brown, M.D., for critical review of the manuscript. This work was supported by the National Institutes of Health grants R01-DK54387 and DK46181 and CTSA Grant UL1 RR024982 and Southwest Medical Foundation.

Received: September 2, 2010
Revised: October 18, 2010
Accepted: October 25, 2010
Published online: December 2, 2010

Web Resources

The URLs for data presented herein are as follows:

Human Genome Variation Society, http://www.hgvs.org/mutnomen/

MERLIN, http://www.sph.umich.edu/csg/abecasis/Merlin/

National Center for Biotechnology Information, http://www.ncbi.nlm.nih.gov/

Online Mendelian Inheritance in Man (OMIM), http://www.ncbi.nlm.nih.gov/Omim/

PLINK, pngu.mgh.harvard.edu/~purcell/plink/

Prochek, http://www.ebi.ac.uk/thornton-srv/software/PROCHECK/

Protein, http://www.ncbi.nlm.nih.gov/protein/

RCSB Protein Databank, http://www.rcsb.org/pdb/explore/explore.do?structureId = 1Z7Q

SNP database, http://www.ncbi.nlm.nih.gov/snp/

University of California, Santa Cruz (UCSC) Genome Browser, http://www.genome.ucsc.edu

References

1. Garg, A., Hernandez, M.D., Sousa, A.B., Subramanyam, L., de Villarreal, L.M., Dos Santos, H.G., and Barboza, O. (2010). An autosomal recessive syndrome of joint contractures, muscular atrophy, microcytic anemia, and panniculitis-associated lipodystrophy. J. Clin. Endocrinol. Metab. *95*, E58–E63.
2. Tanaka, M., Miyatani, N., Yamada, S., Miyashita, K., Toyoshima, I., Sakuma, K., Tanaka, K., Yuasa, T., Miyatake, T., and Tsubaki, T. (1993). Hereditary lipo-muscular atrophy with joint contracture, skin eruptions and hyper-gamma-globulinemia: A new syndrome. Intern. Med. *32*, 42–45.
3. Yamada, S., Toyoshima, I., Mori, S., and Tsubaki, T. (1984). [Sibling cases with lipodystrophic skin change, muscular atrophy, recurrent skin eruptions, and deformities and contractures of the joints. A possible new clinical entity]. Rinsho Shinkeigaku *24*, 703–710.
4. Oyanagi, K., Sasaki, K., Ohama, E., Ikuta, F., Kawakami, A., Miyatani, N., Miyatake, T., and Yamada, S. (1987). An autopsy case of a syndrome with muscular atrophy, decreased subcutaneous fat, skin eruption and hyper gamma-globulinemia: Peculiar vascular changes and muscle fiber degeneration. Acta Neuropathol. *73*, 313–319.
5. Horikoshi, A., Iwabuchi, S., Iizuka, Y., Hagiwara, T., and Amaki, I. (1980). [A case of partial lipodystrophy with erythema, dactylic deformities, calcification of the basal ganglia, immunological disorders, and low IQ level (author's transl)]. Rinsho Shinkeigaku *20*, 173–180.
6. Henderson, C., and Goldbach-Mansky, R. (2010). Monogenic autoinflammatory diseases: New insights into clinical aspects and pathogenesis. Curr. Opin. Rheumatol. *22*, 567–578.
7. Lander, E.S., and Botstein, D. (1987). Homozygosity mapping: A way to map human recessive traits with the DNA of inbred children. Science *236*, 1567–1570.
8. Hildebrandt, F., Heeringa, S.F., Ruschendorf, F., Attanasio, M., Nurnberg, G., Becker, C., Seelow, D., Huebner, N., Chernin, G., Vlangos, C.N., et al. (2009). A systematic approach to mapping recessive disease genes in individuals from outbred populations. PLoS Genet. *5*, e1000353.
9. Abecasis, G.R., Cherny, S.S., Cookson, W.O., and Cardon, L.R. (2002). Merlin—rapid analysis of dense genetic maps using sparse gene flow trees. Nat. Genet. *30*, 97–101.
10. Purcell, S., Neale, B., Todd-Brown, K., Thomas, L., Ferreira, M.A., Bender, D., Maller, J., Sklar, P., de Bakker, P.I., Daly, M.J., et al. (2007). PLINK: A tool set for whole-genome association and population-based linkage analyses. Am. J. Hum. Genet. *81*, 559–575.
11. Agarwal, A.K., Arioglu, E., de Almeida, S., Akkoc, N., Taylor, S.I., Bowcock, A.M., Barnes, R.I., and Garg, A. (2002). *AGPAT2* is mutated in congenital generalized lipodystrophy linked to chromosome 9q34. Nat. Genet. *31*, 21–23.
12. Forster, A., Masters, E.I., Whitby, F.G., Robinson, H., and Hill, C.P. (2005). The 1.9 A structure of a proteasome-11S activator complex and implications for proteasome-PAN/PA700 interactions. Mol. Cell *18*, 589–599.
13. Unno, M., Mizushima, T., Morimoto, Y., Tomisugi, Y., Tanaka, K., Yasuoka, N., and Tsukihara, T. (2002). Structure determination of the constitutive 20S proteasome from bovine liver at 2.75 A resolution. J. Biochem. *131*, 171–173.
14. Case, D.A., Cheatham, T.E., 3rd, Darden, T., Gohlke, H., Luo, R., Merz, K.M., Jr., Onufriev, A., Simmerling, C., Wang, B., and Woods, R.J. (2005). The Amber biomolecular simulation programs. J. Comput. Chem. *26*, 1668–1688.
15. Ponder, J.W., and Case, D.A. (2003). Force fields for protein simulations. Adv. Protein Chem. *66*, 27–85.
16. Luthy, R., Bowie, J.U., and Eisenberg, D. (1992). Assessment of protein models with three-dimensional profiles. Nature *356*, 83–85.
17. Laskowski, R.A., Moss, D.S., and Thornton, J.M. (1993). Main-chain bond lengths and bond angles in protein structures. J. Mol. Biol. *231*, 1049–1067.
18. Wójcik, C., and DeMartino, G.N. (2002). Analysis of *Drosophila* 26S proteasome using RNA interference. J. Biol. Chem. *277*, 6188–6197.
19. Bradford, M.M. (1976). A rapid and sensitive method for the quantitation of microgram quantities of protein utilizing the principle of protein-dye binding. Anal. Biochem. *72*, 248–254.
20. Fabunmi, R.P., Wigley, W.C., Thomas, P.J., and DeMartino, G.N. (2001). Interferon gamma regulates accumulation of the proteasome activator PA28 and immunoproteasomes at nuclear PML bodies. J. Cell Sci. *114*, 29–36.
21. Rivett, A.J., and Hearn, A.R. (2004). Proteasome function in antigen presentation: Immunoproteasome complexes, peptide production, and interactions with viral proteins. Curr. Protein Pept. Sci. *5*, 153–161.
22. Bochtler, M., Ditzel, L., Groll, M., Hartmann, C., and Huber, R. (1999). The proteasome. Annu. Rev. Biophys. Biomol. Struct. *28*, 295–317.
23. Kloetzel, P.M. (2001). Antigen processing by the proteasome. Nat. Rev. Mol. Cell Biol. *2*, 179–187.
24. Groll, M., Heinemeyer, W., Jager, S., Ullrich, T., Bochtler, M., Wolf, D.H., and Huber, R. (1999). The catalytic sites of 20S proteasomes and their role in subunit maturation: A mutational and crystallographic study. Proc. Natl. Acad. Sci. USA *96*, 10976–10983.
25. Toes, R.E., Nussbaum, A.K., Degermann, S., Schirle, M., Emmerich, N.P., Kraft, M., Laplace, C., Zwinderman, A., Dick, T.P., Muller, J., et al. (2001). Discrete cleavage motifs of constitutive and immunoproteasomes revealed by quantitative analysis of cleavage products. J. Exp. Med. *194*, 1–12.
26. Gaczynska, M., Rock, K.L., Spies, T., and Goldberg, A.L. (1994). Peptidase activities of proteasomes are differentially regulated by the major histocompatibility complex-encoded

genes for LMP2 and LMP7. Proc. Natl. Acad. Sci. USA *91*, 9213–9217.

27. Diez-Rivero, C.M., Lafuente, E.M., and Reche, P.A. (2010). Computational analysis and modeling of cleavage by the immunoproteasome and the constitutive proteasome. BMC Bioinformatics *11*, 479.
28. Fehling, H.J., Swat, W., Laplace, C., Kuhn, R., Rajewsky, K., Muller, U., and von Boehmer, H. (1994). MHC class I expression in mice lacking the proteasome subunit LMP-7. Science *265*, 1234–1237.
29. Nussbaum, A.K., Rodriguez-Carreno, M.P., Benning, N., Botten, J., and Whitton, J.L. (2005). Immunoproteasome-deficient mice mount largely normal CD8+ T cell responses to lymphocytic choriomeningitis virus infection and DNA vaccination. J. Immunol. *175*, 1153–1160.
30. Tu, L., Moriya, C., Imai, T., Ishida, H., Tetsutani, K., Duan, X., Murata, S., Tanaka, K., Shimokawa, C., Hisaeda, H., et al. (2009). Critical role for the immunoproteasome subunit LMP7 in the resistance of mice to *Toxoplasma gondii* infection. Eur. J. Immunol. *39*, 3385–3394.
31. Muchamuel, T., Basler, M., Aujay, M.A., Suzuki, E., Kalim, K.W., Lauer, C., Sylvain, C., Ring, E.R., Shields, J., Jiang, J., et al. (2009). A selective inhibitor of the immunoproteasome subunit LMP7 blocks cytokine production and attenuates progression of experimental arthritis. Nat. Med. *15*, 781–787.